Revealing the second harmonic generation in a femtosecond laser-driven cluster-based plasma by analyzing shapes of Ar XVII spectral lines

Eugene Oks, Elisabeth Dalimier, Anatoly Faenov, Tatiana Pikuz, Yuji Fukuda, Alexander Andreev, James Koga, Hironao Sakaki, Hideyuki Kotaki, Alexander Pirozhkov, et al.

Revealing the second harmonic generation in a femtosecond laser-driven cluster-based plasma by analyzing shapes of Ar XVII spectral lines

Eugene Oks,[1,*] Elisabeth Dalimier,[2] Anatoly Faenov,[3,4] Tatiana Pikuz,[3,4] Yuji Fukuda,[5] Alexander Andreev,[6,9] James Koga,[5] Hironao Sakaki,[5] Hideyuki Kotaki,[5] Alexander Pirozhkov,[5] Yukio Hayashi,[5] Igor Skobelev,[4,7] Sergei Pikuz,[4,7] Tetsuya Kawachi,[5] Masaki Kando,[5] Kiminori Kondo,[5] Alexei Zhidkov,[8] and Ryosuke Kodama[3,8]

[1]*Physics Dept,. 206 Allison Lab., Auburn University, Auburn, Alabama 36849, USA*
[2]*LULI-UPMC Univ Paris 06: Sorbonne Universites ; CNRS, Ecole Polytechnique,CEA:Universite Paris-Saclay –F-75252 Paris Cedex 05, France*
[3]*Institute for Academic Initiatives, Osaka University, Suita, Osaka, 565-0871, Japan*
[4]*Joint Institute for High Temperatures, Russian Academy of Sciences, ul. Izhorskaya 13/19, Moscow, 125412 Russia*
[5]*Quantum Beam Science Directorate, Japan Atomic Energy Agency, 619-0215 Kyoto, Japan*
[6]*Max Born Institute, Berlin 12489, Max-Born str.2a, Berlin, Germany*
[7]*National Research Nuclear University MEPhI (Moscow Engineering Physics Institute), Moscow 115409, Russia*
[8]*PPC Osaka University and JST, CREST, 2-1, Yamadaoka, Suita, Osaka 565-0871, Japan*
[9]*ELI-ALPS, Szeged H-6720, Hungary*
[*]*goks@physics.auburn.edu*

Abstract: We present experiments dealing with a femtosecond laser-driven cluster-based plasma, where by analyzing the nonlinear phenomenon of satellites of spectral lines of Ar XVII, we revealed the nonlinear phenomenon of the generation of the second harmonic of the laser frequency. For performing this analysis we developed new results in the theory of satellites of spectral lines. From such lineshape analysis we found, in particular, that the efficiency of converting the short (40 fs) intense ($3x10^{18}$ W/cm^2) incident laser light into the second harmonic was 2%. This result is in the excellent agreement with the 2-Dimensional Particle-In-Cell (2D PIC) simulation that we also performed. There is also an order of magnitude agreement between the thresholds for the SHG found from the line shape analysis and from the 2D PIC simulations.

OCIS codes: (020.2649) Strong field laser physics; (320.2250) Femtosecond phenomena; (190.2620) Harmonic generation and mixing; (350.5400) Plasmas; (020.3690) Line shapes and shifts.

References and links

1. V. E. Zakharov, S. L. Musher, and A. M. Rubenchik, "Hamiltonian approach to the description of non-linear plasma phenomena," Phys. Rep. **129**(5), 285–366 (1985).
2. V. N. Tsytovich and D. ter Haar, *Lectures on Non-linear Plasma Kinetikcs*. XI, Springer Series on Atoms and Plasmas, v.17 (Springer, 1995).
3. R. Boyd, *Nonlinear Optics* (Academic Press, 2008).
4. E. Esarey, A. Tung, P. Sprangle, D. Umstadter, and X. Liu, "Nonlinear analysis of relativistic harmonic generation by intense lasers in plasmas," IEEE Trans. Plasma Sci. **21**(1), 95–104 (1993).
5. C. Bula, K. T. McDonald, E. J. Prebys, C. Bamber, S. Boege, T. Kotseroglou, A. C. Melissinos, D. D. Meyerhofer, W. Ragg, D. L. Burke, R. C. Field, G. Horton-Smith, A. C. Odian, J. E. Spencer, D. Walz, S. C. Berridge, W. M. Bugg, K. Shmakov, and A. W. Weidemann, "Observation of nonlinear effects in Compton scattering," Phys. Rev. Lett. **76**(17), 3116–3119 (1996).
6. V. Malka, A. Modena, Z. Najmudin, A. E. Dangor, C. E. Clayton, K. A. Marsh, C. Joshi, C. Danson, D. Neely, and F. N. Walsh, "Second harmonic generation and its interaction with relativistic plasma waves driven by forward Raman instability in underdense plasmas," Phys. Plasmas **4**(4), 1127–1131 (1997).
7. A. Chen, A. Maksimchuk, and D. Umstadter, "Experimental observation of relativistic nonlinear Thomson scattering," Nature **396**(6712), 653–659 (1998).

#250983 Received 29 Sep 2015; revised 19 Nov 2015; accepted 20 Nov 2015; published 3 Dec 2015

8. S. L. Rolston and W. D. Phillips, "Nonlinear and quantum atom optics," Nature **416**(6877), 219–224 (2002).
9. N. Dudovich, D. Oron, and Y. Silberberg, "Single-pulse coherently controlled nonlinear Raman spectroscopy and microscopy," Nature **418**(6897), 512–514 (2002).
10. C. Thaury, F. Quéré, J.-P. Geindre, A. Levy, T. Ceccotti, P. Monot, M. Bougeard, F. Réau, P. d'Oliveira, P. Audebert, R. Marjoribanks, and Ph. Martin, "Plasma mirrors for ultrahigh-intensity optics," Nat. Phys. **3**(6), 424–429 (2007).
11. Y. Nomura, R. Hörlein, P. Tzallas, B. Dromey, S. Rykovanov, Zs. Major, J. Osterhoff, S. Karsch, L. Veisz, M. Zepf, D. Charalambidis, F. Krausz, and G. D. Tsakiris, "Attosecond phase locking of harmonics emitted from laser-produced plasmas," Nat. Phys. **5**(2), 124–128 (2009).
12. T. Popmintchev, M.-C. Chen, P. Arpin, M. M. Murname, and H. C. Kapteyn, "The attosecond nonlinear optics of bright X-ray generation," Nat. Photonics **4**(12), 822–832 (2010).
13. N. D. Powers, I. Ghebregziabher, G. Golovin, C. Liu, S. Chen, S. Banerjee, J. Zhang, and D. P. Umstadter, "Quasi-monoenergetic and tunable X-rays from a laser-driven Compton light source," Nat. Photonics **8**(1), 28–31 (2013).
14. Y. Wang, S. Wang, E. Oliva, L. Li, M. Berrill, L. Yin, J. Nejdl, B. M. Luther, C. Proux, T. T. T. Le, J. Dunn, D. Ros, Ph. Zeitoun, and J. J. Rocca, "Gain dynamics in a soft X-ray laser amplifier perturbed by a strong injected X-ray field," Nat. Photonics **8**(5), 381–384 (2014).
15. L. M. Chen, W. C. Yan, D. Z. Li, Z. D. Hu, L. Zhang, W. M. Wang, N. Hafz, J. Y. Mao, K. Huang, Y. Ma, J. R. Zhao, J. L. Ma, Y. T. Li, X. Lu, Z. M. Sheng, Z. Y. Wei, J. Gao, and J. Zhang, "Bright betatron X-ray radiation from a laser-driven-clustering gas target," Sci. Rep. **3**, 1912 (2013).
16. D. I. Blochinzew, "Zur Theorie des Starkeffektes im Zeitveränderlichen Feld," Phys. Z. Sow. Union **4**, 501–515 (1933).
17. Ya. B. Zel'dovich, "The quasienergy of a quantum-mechanical system subjected to a periodic action," Sov. Phys. JETP **24**, 1006–1008 (1967).
18. I. Ritus, "Shift and splitting of atomic energy levels by the field of an electromagnetic wave," Sov. Phys. JETP **24**, 1041–1044 (1967).
19. T. D. Donnelly, T. Ditmire, K. Neuman, M. D. Perry, and R. W. Falcone, "High-order harmonic generation in atom clusters," Phys. Rev. Lett. **76**(14), 2472–2475 (1996).
20. S. V. Bulanov, T. Zh. Esirkepov, J. Koga, and T. Tajima, "Interaction of Electromagnetic Waves with Plasma in the Radiation-Dominated Regime," Plasma Phys. Rep. **30**(3), 196–213 (2004).
21. S. V. Fomichev, D. F. Zaretsky, D. Bauer, and W. Becker, "Classical molecular-dynamics simulations of laser-irradiated clusters: Nonlinear electron dynamics and resonance-enhanced low-order harmonic generation," Phys. Rev. A **71**(1), 013201 (2005).
22. V. S. Rastunkov and V. P. Krainov, "Relativistic dipole and non-relativistic quadrupole generation of the second harmonic at the irradiation of atomic clusters by the femtosecond laser pulses," Laser Phys. Lett. **3**(8), 392–395 (2006).
23. V. S. Rastunkov and V. P. Krainov, "Mechanisms for second harmonic generation in the interaction of a superintense ultrashort laser pulse with cluster plasma," Laser Phys. Lett. **3**, 3920395 (2006).
24. M. Kundu, S. V. Popruzhenko, and D. Bauer, "Harmonic generation from laser-irradiated clusters," Phys. Rev. A **76**(3), 033201 (2007).
25. Y. Fukuda, A. Ya. Faenov, T. Pikuz, M. Kando, H. Kotaki, I. Daito, J. Ma, L. M. Chen, T. Homma, K. Kawase, T. Kameshima, T. Kawachi, H. Daido, T. Kimura, T. Tajima, Y. Kato, and S. V. Bulanov, "Soft X-ray source for nanostructure imaging using femtosecond-laser-irradiated clusters," Appl. Phys. Lett. **92**(12), 121110 (2008).
26. H. Kiriyama, M. Mori, Y. Nakai, T. Shimomura, H. Sasao, M. Tanoue, S. Kanazawa, D. Wakai, F. Sasao, H. Okada, I. Daito, M. Suzuki, S. Kondo, K. Kondo, A. Sugiyama, P. R. Bolton, A. Yokoyama, H. Daido, S. Kawanishi, T. Kimura, and T. Tajima, "High temporal and spatial quality petawatt-class Ti:sapphire chirped-pulse amplification laser system," Opt. Lett. **35**(10), 1497–1499 (2010).
27. J. Colgan, J. Abdallah, Jr., A. Ya. Faenov, T. A. Pikuz, I. Yu. Skobelev, Y. Fukuda, Y. Hayashi, A. Pirozhkov, K. Kawase, T. Shimomura, H. Kiriyama, Y. Kato, S. V. Bulanov, and M. Kando, "Observation and modeling of high resolution spectral features of the inner-shell X-ray emission produced by 10^{-10} contrast femtosecond-pulse laser irradiation of argon clusters," High Energy Density Phys. **7**(2), 77–83 (2011).
28. A. S. Boldarev, V. A. Gasilov, A. Ya. Faenov, Y. Fukuda, and K. Yamakawa, "Gas-cluster targets for femtosecond laser interaction: Modeling and optimization," Rev. Sci. Instrum. **77**(8), 083112 (2006).
29. S. Jinno, Y. Fukuda, H. Sakaki, A. Yogo, M. Kanasaki, K. Kondo, A. Ya. Faenov, I. Yu. Skobelev, T. A. Pikuz, A. S. Boldarev, and V. A. Gasilov, "Characterization of submicron-sized CO2 clusters formed with a supersonic expansion of a mixed-gas using a three-staged nozzle," Appl. Phys. Lett. **102**(16), 164103 (2013).
30. S. Jinno, Y. Fukuda, H. Sakaki, A. Yogo, M. Kanasaki, K. Kondo, A. Ya. Faenov, I. Yu. Skobelev, T. A. Pikuz, A. S. Boldarev, and V. A. Gasilov, "Mie scattering from submicron-sized CO_2 clusters formed in a supersonic expansion of a gas mixture," Opt. Express **21**(18), 20656–20674 (2013).
31. A. Ya. Faenov, S. A. Pikuz, A. I. Erko, B. A. Bryunetkin, V. M. Dyakin, G. V. Ivanenkov, A. R. Mingaleev, T. A. Pikuz, V. M. Romanova, and T. A. Shelkovenko, "High-performance X-ray spectroscopic devices for plasma microsources investigations," Phys. Scr. **50**(4), 333–338 (1994).
32. F. Blasco, C. Stenz, F. Salin, A. Ya. Faenov, A. I. Magunov, T. A. Pikuz, and I. Yu. Skobelev, "Portable, tunable, high-luminosity spherical crystal spectrometer with X- Ray charge couple device, for high-resolution X-Ray spectromicroscopy of clusters, heated by femtosecond laser pulses," Rev. Sci. Instrum. **72**(4), 1956 (2001).

#250983 Received 29 Sep 2015; revised 19 Nov 2015; accepted 20 Nov 2015; published 3 Dec 2015

33. F. B. Rosmej and A. Ya. Faenov, "New innershell phenomena from Rydberg series of highly charged ions," Phys. Scr. T **173**, 106–107 (1997).
34. F. B. Rosmej, A. Ya. Faenov, T. A. Pikuz, F. Flora, P. Di Lazzaro, T. Letardi, A. Grilli, A. Reale, L. Palladino, G. Tomassetti, A. Scafati, and L. Reale, "Line formation of high intensity Heb Rydberg dielectronic satellites 1s3lnl' in dense laser-produced plasmas," J. Phys. B. Letters **31**(21), L921–L931 (1998).
35. F. B. Rosmej, U. N. Funk, M. Geissel, D. H. H. Hoffmann, A. Tauschwitz, A. Ya. Faenov, T. A. Pikuz, I. Yu. Skobelev, F. Flora, S. Bollanti, P. Di. Lazzaro, T. Letardi, A. Grilli, L. Palladino, A. Reale, G. Tomassetti, A. Scafati, L. Reale, T. Auguste, P. D'Oliveira, S. Hulin, P. Monot, A. Maksimchuk, S. A. Pikuz, D. Umstadter, M. Nantel, R. Bock, M. Dornik, M. Stetter, S. Stowe, V. Yakushev, M. Kulisch, and N. Shilkin, "X-Ray radiation from ions with K-shell vacancies," J. Quant. Spestrosc. Rad. Transfer **65**(4–6), 477–499 (2000).
36. F. B. Rosmej, D. H. H. Hoffmann, M. Geißel, M. Roth, P. Pirzadeh, A. Ya. Faenov, T. A. Pikuz, I. Yu. Skobelev, and A. I. Magunov, "Advanced X-ray diagnostics based on an observation of high-energy Rydberg transitions from autoionizing levels in dense laser-produced plasmas," Phys. Rev. A **63**(6), 063409 (2001).
37. M. E. Sherrill, J. Abdallah, Jr., G. Csanak, E. S. Dodd, Y. Fukuda, Y. Akahane, M. Aoyama, N. Inoue, H. Ueda, K. Yamakawa, A. Ya. Faenov, A. I. Magunov, T. A. Pikuz, and I. Yu. Skobelev, "Spectroscopic characterization of an ultrashort-pulse-laser-driven Ar cluster target incorporating both Boltzmann and particle-in-cell models," Phys. Rev. E Stat. Nonlin. Soft Matter Phys. **73**(6), 066404 (2006).
38. P. Maine, D. Strickland, P. Bado, M. Pessot, and G. Mourou, "Generation of ultrahigh peak power pulses by chirped pulse amplification," IEEE J. Quantum Electron. **24**(2), 398–403 (1988).
39. A. I. Akhiezer and R. V. Polovin, "Theory of Wave Motion of an Electron. Plasma," Sov. Phys. JETP **3**, 696–705 (1956).
40. W. Lünow, "On the relativistic non-linear interaction of cold plasma with electro-magnetic waves," Plasma Phys. **10**(9), 879–897 (1968).
41. S. Guérin, P. Mora, J. C. Adam, A. Heron, and G. Laval, "Propagation of ultraintense laser pulses through overdense plasma layers," Phys. Plasmas **3**(7), 2693–2701 (1996).
42. E. Oks, "Spectroscopy of plasmas containing quasimonochromatic electric fields," Sov. Phys. Dokl. **29**, 224–226 (1984).
43. E. Oks, *Plasma Spectroscopy: The Influence of Microwave and Laser Fields* (Springer, 1995).
44. V. P. Gavrilenko and E. Oks, "New method of spatially-resolved measurements of the amplitude-angular distribution of a low-frequency plasma turbulence," Proc. 17th Int. Conf. on Phenom. in Ionized Gases (Budapest, Hungary) pp. 1081–1083 (1985).
45. V. P. Gavrilenko, E. Oks, and V. A. Rantsev-Kartinov, "Observation and analysis of oscillatory electric fields in the peripheral plasma in a tokamak on the basis of a new spectroscopic effect," JETP Lett. **44**, 404–408 (1986).
46. S. Djurović, M. Ćirišan, A. V. Demura, G. V. Demchenko, D. Nikolić, M. A. Gigosos, and M. A. González, "Measurements of Hβ Stark central asymmetry and its analysis through standard theory and computer simulations," Phys. Rev. E Stat. Nonlin. Soft Matter Phys. **79**(4 Pt 2), 046402 (2009).
47. A. V. Demura, G. V. Demchenko, and D. Nikolic, "Multiparametric dependence of hydrogen Stark profiles asymmetry," Eur. Phys. J. D **46**(1), 111–127 (2008).
48. C. Thaury and F. Quere, "High-order harmonic and attosecond pulse generation on plasma mirrors: basic mechanisms," J. Phys. B **43**(21), 213001 (2010).
49. A. Andreev and K. Platonov, "Generation of electron nanobunches and short wavelength radiation upon reflection of a relativistic intensity laser pulse from a finite size target," Opt. Spectrosc. **114**(5), 788–797 (2013).
50. J. Braenzel, A. Andreev, M. Schnürer, S. Steinke, K. Platonov, G. Priebe, and W. Sandner, "Sub-structure of laser generated harmonics reveals plasma dynamics of a relativistically oscillating mirror," Phys. Plasmas **20**(8), 083109 (2013).

1. Introduction

Various nonlinear phenomena had been observed in optics and plasma physics [1–3] increasing laser intensities and shortening of the pulses, new nonlinear phenomena occur involving many of fields of physics [4–15].

In atomic physics, the interaction of the simplest atoms – hydrogen atoms – with a monochromatic electric field (e.g., a laser field) $\mathbf{E}(t) = \mathbf{E}_1 \cos(\omega t)$ results in a nonlinear phenomenon in the spectrum of the radiation known as Blochinzew's satellites [16]. Namely, a hydrogen spectral line splits up in a series of satellites at the distances (counted from the unperturbed frequency ω_0 of the spectral line) $\Delta\omega = \pm p\omega$, where $p = 0, 1, 2, \ldots$.

As early as in 1933, Blochinzew showed that the intensity I_p of the satellite at the frequency $p\omega$ is proportional to the square of the Bessel function $J_p^2(kE_1/\omega)$, where k = const. At relatively small fields, such as $kE_1/\omega << 1$, one gets $J_p^2(kE_1/\omega) = (kE_1/\omega)^{2p}$, so that practically only the first satellite (p = 1) can be observed and its intensity is linear with respect to the energy density of the field (I_1 is proportional to E_1^2). However, as the field increases, due to the oscillatory nature of the Bessel functions, the dependence of the satellite intensity

#250983 Received 29 Sep 2015; revised 19 Nov 2015; accepted 20 Nov 2015; published 3 Dec 2015

on the energy density of the field becomes highly nonlinear. We note that Blochinzew's result was actually the first example of a more general phenomenon later called "quasienergy spectrum" and "quasienergy harmonics", as introduced by Zeldovich [17] and Ritus [18] in 1964 (Fig. 1(a), 1(b)).

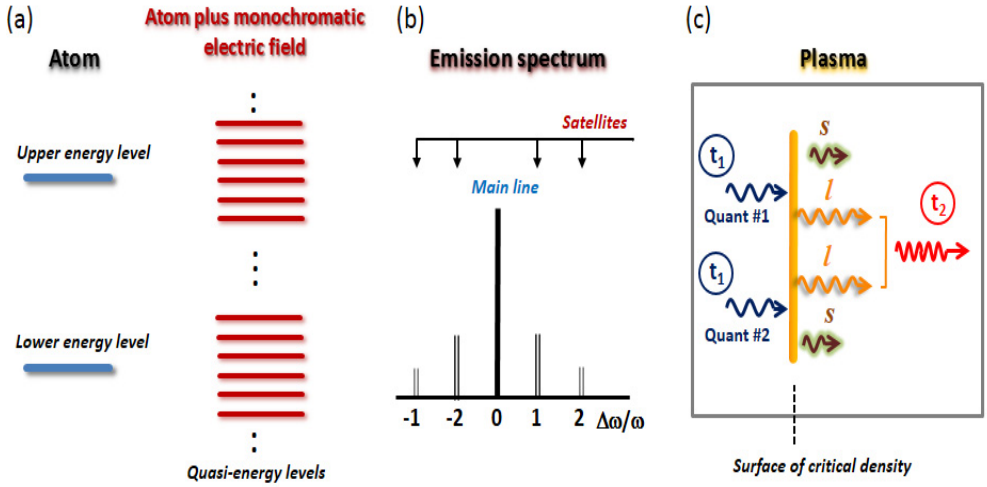

Fig. 1. Schematic of interlinked nonlinear processes. (a) Quasienergy States (QS) of the combined system "atom + electric field $E(t) = E_0 \cos\omega t$". Each atomic/ionic energy level "splits up" into generally infinite number of QS, separated from each other by $\hbar\omega$. Only few QS are shown (by red lines). The presence of many other QS (of generally infinite amount) is symbolically indicated by dots, like in the sequence $\pm \hbar\omega, \pm 2\hbar\omega, \pm 3\hbar\omega, \ldots$.(b) The spectrum of radiative transitions between QS shows satellites at $\pm \omega, \pm 2\omega, \ldots$ (in the frequency scale) in addition to the main spectral line. While there is generally an infinite number of QS, practically only a finite number of satellites is observed. (c) Schematic representation of one of the mechanisms of the second harmonic generation – just as an illustrative example. The pump wave (t_1) excites both the Langmuir wave (l) and the ion-acoustic wave (s): $t_1 \rightarrow l + s$. Then the predominant process is $l + l \rightarrow t_2$, where two Langmuir waves combine to produce a transverse electromagnetic wave (t_2) at twice the laser frequency.

In the research area of laser-plasma interactions, one of the important phenomena is Harmonic Generation (HG) – for example, the doubling of the laser frequency [3,6,12,19–24]. Mechanisms of HG involve various nonlinear processes, some of which, in particular, for laser interaction with clusters were considered in [19–24]. For example, in the first step, the transverse laser field (t_1) of the frequency ω (the pump wave) excites a longitudinal Langmuir wave (l). At fairly high laser intensity this occurs via a parametric instability – typically as a parametric decay, which is a nonlinear process where the pump wave (t_1) excites both the Langmuir wave (l) and an ion-acoustic wave (s):

$$t_1 \rightarrow l + s. \qquad (1)$$

Parametric instabilities are a common wave-wave interaction. They arise when a nonlinearity such as a pressure gradient couples waves. The physical mechanism is that the pump wave causes oscillations of plasma electrons, which in its turn excite the Langmuir wave and, via the nonlinear coupling – the ion acoustic wave. For this to be possible, the waves must allow frequency and wavenumber matching, which are consequences of energy and momentum conservation. Therefore, the above first step occurs near the surface of the critical electron density

#250983 Received 29 Sep 2015; revised 19 Nov 2015; accepted 20 Nov 2015; published 3 Dec 2015

$$N_{ec} = \frac{m_e \omega}{4\pi e^2}, \tag{2}$$

which is the surface where the laser frequency ω is equal to the plasma electron frequency ω_{pe} of the Langmuir wave.

The second step requires at least one of the two nonlinear processes. The predominant process is

$$l + l \rightarrow t_2, \tag{3}$$

where two Langmuir waves, excited at the first step at the frequency close to the laser frequency, combine to produce a transverse electromagnetic wave (t_2) at twice the laser frequency (Fig. 1(c)). The other possible process is

$$l + t_1 \rightarrow t_2, \tag{4}$$

where the Langmuir wave interacts with the laser radiation pump wave to produce a transverse electromagnetic wave (t_2) at twice the laser frequency. Both nonlinear processes at the second step involve the Langmuir wave at the frequency ω_{pe} close to the laser frequency ω – consequently both processes occur near the surface of the critical density. The above is just an illustrative example – there are also other mechanisms of HG [3,6,12,19–24].

The aim of the present work is to develop a novel advanced way of studying an important nonlinear phenomenon in one area of physics by using a different nonlinear phenomenon from another area of physics. Namely, we present experiments dealing with a femtosecond laser-driven cluster-based plasma, where by analyzing the nonlinear phenomenon of (non-Blochinzew) satellites of spectral lines of Ar XVII, we revealed the nonlinear phenomenon of the generation of the second harmonic of the laser frequency in the plasma produced from clusters. This was made possible due to measurements of the x-ray spectra with a high spectral resolution (λ/δλ~3000) in a rather broad spectral range under the irradiation of clusters at various laser intensities. This provided insights into the nature of radiation processes of clusters irradiated by ultra-high intensity femtosecond laser pulses. Thus, the nonlinear process of the second harmonic generation manifested via the nonlinear process of the spectral lines satellites.

In Sect. 2 we describe the experiment. In Sect. 3 we analyze the experimental results. In Sect. 4 we complement the analysis by PIC simulations. In Sect. 5 we present conclusions.

2. Experiment

The experiments have been performed at Kansai Photon Science Institute, Japan Atomic Energy Agency (KPSI, JAEA, Japan). Two Ti:sapphire laser facilities (wavelength approximately 800 nm) were used. In the first experiment the JLITE-X laser generated 40 fs pulses of the energy of 160 mJ with the contrast of 10^5 and the laser intensity up to $4x10^{17}$ W/cm^2 in vacuum [25]. In the second experiment the J-KAREN laser [26] provided laser pulses with the high contrast of 10^8–10^{10} (with respect to the power; at several picoseconds before the pulse peak. See Fig. 2(d) about the contrast time dependence). The contrast is additionally improved by a saturable absorber inserted between the high-energy CPA oscillator and the stretcher. The ultrafast Pockels cell with the extinction ratio of 200 is applied 500 ps before the main pulse to secure the contrast on the nanosecond time scale. The laser pulse duration was of 40 fs and the pulse energy was of ~800 mJ. The intensity of the laser radiation in the focal spot of the diameter of 30 μm reached 3×10^{18} W/cm^2 in vacuum [27]. The laser beam was focused about 1.5 mm above the nozzle orifice by an off-axis parabola (Fig. 2).

The Ar clusters were created when a gas of a high initial pressure was expanded into vacuum through a specially designed supersonic nozzle [28–30], which consisted of three

#250983 Received 29 Sep 2015; revised 19 Nov 2015; accepted 20 Nov 2015; published 3 Dec 2015

coaxial conical surfaces. The experiments were mainly carried out at the reservoir pressure of 6 MPa of Ar gas, which implies that the mean size of the Ar clusters was ~1.5 μm at the distance of about 1 mm from the edge of the nozzle, where the laser beam was focused (Fig. 2 (a)). With the high contrast of the laser and such a large cluster size, the majority of the Ar clusters were not destroyed by the prepulse until the main laser pulse arrived.

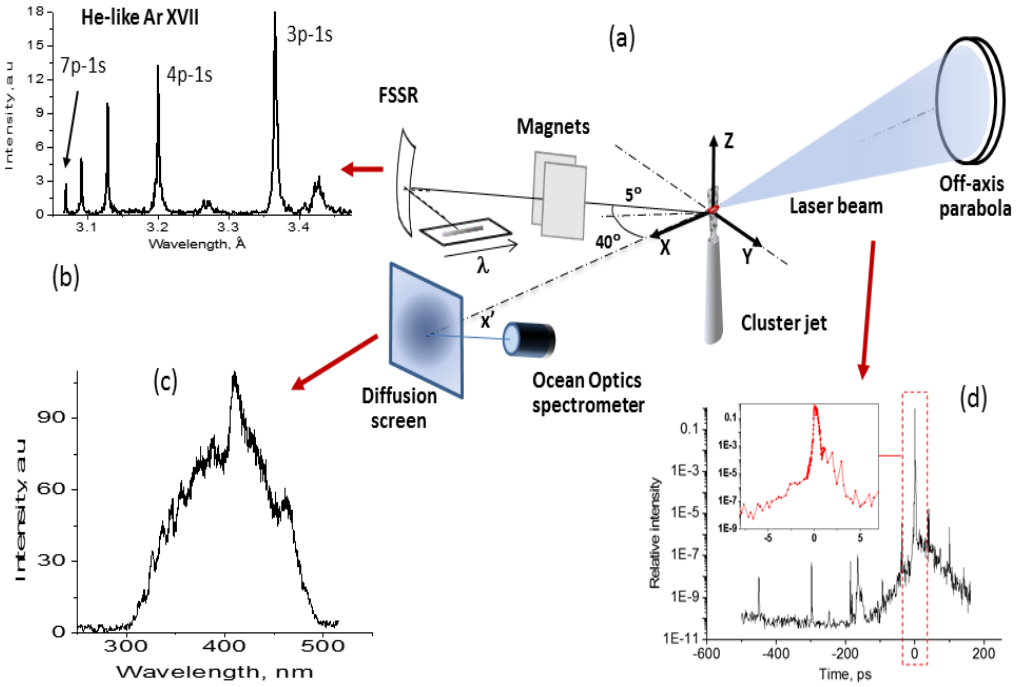

Fig. 2. Schematic experimental setup (a) and a typical X-ray spectrum of Ar cluster plasma in the spectral range 0.305 –0. 35 nm (b), as well as a typical spectrum of the laser beam in the 200 – 500 nm spectral range (c). The laser beam with the contrast shown in (d), ionized Ar clusters and caused nonlinear processes in the cluster plasma. Spectra of Ar XVII were measured by the X-ray spectrometer FSSR. The laser radiation that passed through the cluster plasma was scattered off the screen and spectra of the scattered light in the visible range were measured by the Ocean Optics USB2000 spectrometer.

For high-resolution X-ray spectroscopy measurements a Focusing Spectrometer with Spatial Resolution (FSSR) [31,32] was implemented. The instrument was equipped with a spherically bent quartz (11-20) crystal with the lattice spacing 2d = 4.912 Å and the radius of curvature of R = 150 mm. The crystal was aligned to record K-shell emission spectra of multicharged He-like Ar XVII from the Ly-3 line up to the Ly-7 line in the spectral range of 3.05 – 3.5 Å. The FSSR spectral resolving power was approximately 3000. The X-ray spectra from Ar-cluster plasma were observed at the angle of ~40° to the direction of laser beam propagation. The spherically bent crystal was placed at a distance of 500 mm from the plasma source and was centered at wavelength of 3.25 Å, which corresponds to the Bragg angle of 41.5°. Spectra were recorded on the X-ray Andor DX-440 back-illuminated charge-coupled device (CCD) with the pixel size 13.5 μm, placed at the distance of 537.7 mm from the source. In such configuration, the spatial resolution along the beam propagation was ~70 μm. The X-ray CCD was protected against the exposure to the visible light using two layers of 1 μm thick polypropylene coated from both sides with 0.2 μm Al. The background fogging and crystal fluorescence due to the intense fast electrons were limited using a pair of 0.5 T neodymium-iron-boron permanent magnets that formed a slit of ~15 mm wide in front of the

#250983 Received 29 Sep 2015; revised 19 Nov 2015; accepted 20 Nov 2015; published 3 Dec 2015

crystal (Fig. 2). Using such a magnet system allowed us to drastically reduce the level of the background noise in our experiments.

The rigorous noise level analysis was done in the following way. Obtained raw data was averaged by 5 pixels along the spectral resolution using the standard software. As the spectral resolution of our spectrometer was ~0.19 mA/pxl we estimated that after such a procedure our spectral resolution was ~1 mA. To reduce additionally the background noise, the spectra presented in Fig. 3 were spatially-averaged over the whole volume of the plasma emission. In distinction, spectra presented in Fig. 4 were averaged only by 4 pixels, which allowed us to have spectra with the spatial resolution corresponding to 280 μm. (We note that the spectra presented in Fig. 5 were also spatially-averaged over the whole volume of the plasma emission for reducing the background noise.) After such procedures the level of noise was rather low, as could be seen from Figs. 3-5, and its effect on the analyzed spectra was not significant.

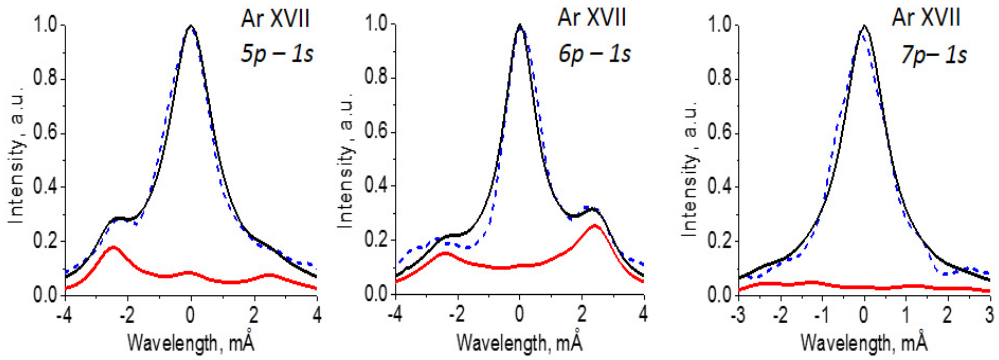

Fig. 3. Comparion of experimental and theoretical spectra of the lines Ar XVII Ly-delta (Ly-5), Ly-epsilon (Ly-6), and Ly-zeta (Ly-7), obtained at laser intensity ~$3x10^{18}$ W/cm^2 (J-KAREN laser facility). Dashed blue – experimental spectra, solid red at the bottom – theoretical spectra from the *bi-chromatic* field region (the field is $E_1\cos(\omega t) + E_2\cos(2\omega t)$, E_1 = 14 GV/cm, E_2 = 7 GV/cm), solid black – total theoretical spectra, including the region of no bi-chromatic field.

The combination of the high luminosity of the FSSR spectrometer with the highly sensitive X-ray CCD allowed measuring the spectrum in each laser shot. A typical part of the obtained spectra is presented in Fig. 2 (for a better contrast, these spectra are the summation of 2 shots). For comparison to the experimental data, a forward processing of the calculated spectra was performed including the filter absorption and the CCD response. Additionally, a polypropylene filter of 6 μm thickness was used to reduce the noise level.

Spectral properties of laser beam scattered by the cluster plasma media were studied in the forward direction. We set for this a polytetrafluoroethylene (PTFE) screen at the distance of 63 cm from the plasma in the direction of the laser beam propagation (See Fig. 2(a)). Such a screen allowed measuring the scattered laser radiation in the angle covering ~ + −13 degrees. Spectra of the scattered laser radiation were measured by the OceanOptics USB2000 spectrometer operated in the spectral range 200 – 500 nm without a fiber outside the vacuum chamber. It measured the radiation scattered off the PTFE screen at ~60 degrees, which passed through a window and was directed to the spectrometer by an Aluminum mirror. The total distance from the screen to the spectrometer was ~1.2 m. To avoid a stray light caused by the laser, the scattered radiation passed through a dichroic beam splitter reflecting out the laser light. A typical scattered laser beam spectrum is presented in Fig. 2(c) and it is clearly seen that the 2ω laser light dominated it.

It should be noted that observed plasma emission spectra contained not only resonance series of He-like Argon but also their dielectronic satellites. The observation of such

#250983 Received 29 Sep 2015; revised 19 Nov 2015; accepted 20 Nov 2015; published 3 Dec 2015

transitions, generally speaking, gives an additional possibility to diagnose plasmas (see, e.g., Rosmej et al [33–36]). However, because we observed time-integrated spectra, we can obtain by this method only time-averaged plasma parameters. For effects considered in the present paper only plasma parameters corresponding to the heating time interval would be relevant, but obtaining them would require a time-resolved X-ray plasma emission. Indeed, the radiation time of resonance lines of He-like Ar lines and their dielectronic satellites is about several ps (see, Sherill et al. [37]), but the laser pulse duration, responsible for the generation of the second harmonic, is 65 fs. Unfortunately, currently it is impossible to measure simultaneously 2ω "laser" satellites and dielectronic satellites (emitted for much longer time than the 2ω "laser" satellites) with tens femtosecond time resolution.

3. Experimental results and their analysis

Experimental spatially-integrated spectra of the lines Ar XVII Ly-delta (Ly-5), Ly-epsilon (Ly-6), and Ly-zeta (Ly-7), obtained at the laser intensity $3x10^{18}$ W/cm^2 (the pulse duration 40 fs) are presented in Fig. 3. Experimental profiles of the lines Ly-5 and especially Ly-6 exhibit satellites separated from the line center by $2\omega[\lambda_n^2/(2\pi c)]$, where ω is the laser frequency and λ_n is the unperturbed wavelength of the Ly-n line of Ar XVII. In other words, the experimental spectra show satellites at the frequencies ± 2ω (counted from the line center in the frequency scale), but do not show satellites at the frequencies ± ω. If the emission would be only from the plasma region where only the wave t_2 exists, it would be fairly easy to interpret the experimental spectra. But this scenario could occur only if the emission originates from the overdense plasma at the density N_e such that

$$N_{ec} < N_e < 4N_{ec}, \tag{5}$$

which for the laser frequency ω = $2.4x10^{15}$ s^{-1} translates into the interval $1.8x10^{21}$ cm^{-3} < N_e < $7.2x10^{21}$ cm^{-3}. For clarity: in large clusters the laser radiation pump wave t_1 cannot penetrate the plasma of the density higher than N_{ec}, while its second harmonic t_2 can – but only as long as the density does not exceed $4N_{ec}$. We also note that for sufficiently high laser intensity I, due to relativistic effects, the so-called "relativistic" critical electron density N_{ecr} might become higher than N_{ec} [38–40]. For the linearly-polarized laser radiation, according to paper [41], $N_{ecr} = (\pi a/4)\, N_{ec}$, where $a = \lambda(\mu m)\, [I(W/cm^2)/(1.37x10^{18})]^{1/2}$. At I = $3x10^{18}$ W/cm^2, the formally-calculated N_{ecr} does not exceed N_{ec}, meaning that the threshold for concept of the relativistic critical density to become effective has not been reached.

However, the broadening of the experimental Ar XVII Ly-lines delta, epsilon, and zeta corresponds to noticeably lower densities and thus does not support such scenario. Therefore we have to consider the situation where the observed spectra are formed under the joint action of a relatively strong wave t_1 at the frequency ω and a weaker wave t_2 at the frequency 2ω. (The second harmonic generation produces a wave weaker than the pump wave.) This situation presents quite a challenge for interpreting the experimental spectra. Indeed, it would seem that the stronger wave t_1 at the frequency ω should produce relatively strong satellites at the frequencies ± ω; however, these satellites are not observed.

It is well known that in a high density plasma Rydberg high-n ionic states are not realized due to the Debye screening or the small distance between ions. It is possible to estimate this effect by using hydrogenic wavefunctions for description of Rydberg levels. In this approximation the radius of nl-orbital R_{nl} can be calculated by the simple formula $R_{nl} = [3n^2 - l(l+1)]a_0/(2Z)$ (a_0 is the Bohr radius and Z is the spectroscopic number). For the existence of nl-level it is necessary to satisfy the condition $R_{nl} < \min\{R_D, R_i\}$, where R_D is the Debye radius and R_i is the distance between ions. It can be seen that even at the electron temperature T_e = 100 eV levels of Ar XVII with n < 8 exist for the electron density up to $6x10^{21}$ cm^{-3}. If the electron temperature is higher, more excited levels with n = 8 – 10 must exist in this density region.

#250983 Received 29 Sep 2015; revised 19 Nov 2015; accepted 20 Nov 2015; published 3 Dec 2015

At the electron densities ~10^{21} cm^{-3}, Stark broadening of the highly-excited lines Ar XVII Ly-7, Ly-6, and even Ly-5 is practically the same as for hydrogenic systems. This is because the Stark broadening scales as ~n^2 while the fine structure splitting scales as ~$1/n^3$. So, the ratio of the Stark broadening to the fine structure scales as ~n^5. Therefore there exists a threshold value of n, starting from which the spectral lines become essentially hydrogenic. In the conditions of our experiments, this threshold value is n = 5: the Ar XVII lines from n = 5, 6, 7 (and higher) are essentially hydrogenic, while the Ar XVII lines from n = 3 and 4 are not.

While the theory of satellites under the action of a monochromatic field at some frequency ω was developed for an isolated lateral Stark component of a hydrogenic line by Blochinzew [16] and for real, multicomponent hydrogenic lines in [42,43], there was no theory of satellites under a bi-chromatic field, such as a relatively strong wave t_1 at the frequency ω and a weaker wave t_2 at the frequency 2ω. Thus, first of all, we had to develop such theory.

Under a *monochromatic* field, the intensity of each satellite is expressed through just one Bessel function, as follows. The spontaneous emission spectrum of a hydrogenic system under a monochromatic field $E(t) = E_1\cos(\omega t)$ is controlled by the Fourier expansion of the product of the reduced wave functions

$$\Phi^*_{n_\alpha\alpha}\Phi_{n_\beta\beta} = \exp(ix\varepsilon_1 \sin\omega t) = \sum_{p=-\infty}^{\infty} J_p(x\varepsilon_1)\exp(ip\omega t), \tag{6}$$

as shown by Blokhinzew [16]. Here x is the constant of the linear Stark effect, characterizing this Stark component:

$$x = n_\alpha(n_1 - n_2)_\alpha - n_\beta(n_1 - n_2)_\beta, \tag{7}$$

n_1, n_2 being the parabolic quantum numbers, and n being the principal quantum numbers of the upper (subscript α) and lower (subscript β) Stark sublevels involved in the radiative transition; ε_1 is the following dimensionless parameter

$$\varepsilon_1 = 3\hbar E_1 / (2Z_{eff} m_e e\omega), \tag{8}$$

where Z_{eff} is the effective charge perceived by the outer electron (Z_{eff} = 17 for Ar XVII). Therefore the intensity I_p of the satellite at the frequency pω counted from the unperturbed frequency ω_0 of the spectral line (p = = 0, ± 1, ± 2, …), is

$$I_p = \sum_x j_x \left[J_{p-2s}(x\varepsilon_1)\right]^2, \tag{9}$$

where j_x are the relative intensities of the Stark components.

In distinction, in a *bi-chromatic* field the intensity I_p of the satellite at the frequency pω counted from the unperturbed frequency ω_0 of the spectral line is expressed through a sum of products of two different Bessel functions and the number of terms in the sum is generally infinite, as follows. In a bi-chromatic field $E(t) = E_1\cos(\omega t) + E_2\cos(2\omega t)$, the right side of Eq. (6) becomes

$$\Phi^*_{n_\alpha\alpha}\Phi_{n_\beta\beta} = \exp\left[ix(\varepsilon_1 \sin\omega t + \varepsilon_2 \sin 2\omega t)\right], \tag{10}$$

where

$$\varepsilon_2 = \frac{3\hbar E_2}{2Z_{eff} m_e e(2\omega)}, \tag{11}$$

This leads to the following expression for the satellite intensity I_p

#250983 Received 29 Sep 2015; revised 19 Nov 2015; accepted 20 Nov 2015; published 3 Dec 2015

$$I_p = \sum_x j_x \left[\sum_{s=-\infty}^{\infty} J_s(x\varepsilon_2) J_{p-2s}(x\varepsilon_1) \right]^2, \tag{12}$$

which is controlled by the two (rather than one) dimensionless parameters: ε_1 defined by Eq. (8) and ε_2 defined by Eq. (11).

There was also no theory of satellites for *central* Stark components (the components for which x = 0 in Eq. (7)) – whether in a monochromatic or in a bi-chromatic field. The previous theories [16,42,43] in a monochromatic field, as well as the newly developed here theory in a bi-chromatic field, relate to *lateral* Stark components. Ly-n lines with even values of n have central Stark components. So, we had to develop also a theory of satellites for central Stark components – because at the fairly high laser intensity in the present experiments the satellites of the central Stark component of the Ly-6 line cannot be neglected.

For *central* Stark components (x = 0), the instantaneous Stark shift, being quadratic with respect to the instantaneous electric field, is proportional to $[E_1\cos(\omega t)]^2 = E_1^2(1 + \cos 2\omega t)/2$. Therefore, the right side of Eq. (6) becomes

$$\Phi^*_{n_\alpha \alpha} \Phi_{n_\beta \beta} = \exp\left[i\varepsilon_{quadr} \sin 2\omega t) \right], \tag{13}$$

where

$$\varepsilon_{quadr} = \frac{n^4(17n^2 - 9m^2 + 19)a_0^3 E_1^2}{64\hbar Z_{eff}^4 \omega}. \tag{14}$$

Here m is the magnetic quantum number of the Stark sublevels, involved in the emission of the central component, and a_0 is the Bohr radius. The Fourier expansion of the right side of Eq. (13) leads to the following result for the central component contribution $I_{c,2p}$ to the intensity of the satellite at the frequency 2pω counted from the unperturbed frequency ω_0 of the spectral line (p = 0, ± 1, ± 2, …)

$$I_{c,2p} = j_c \left[J_p(\varepsilon_{quadr}) \right]^2, \tag{15}$$

where j_c is the relative intensity of the central Stark component.

The primary task in interpreting the experimental spectra, based on these newly developed theories, was to find a pair (or pairs) of ε_1 and ε_2 satisfying the following criterion: the intensity I_2 of the 2nd satellite significantly exceeds the intensity I_1 of the 1st satellite. It turned out that if in a particular laser shot the satellites are observed only in one spectral line, then there are several pairs of ε_1 and ε_2 satisfying the criterion, thus making it impossible to select a single pair of ε_1 and ε_2.

However, if in a particular laser shot the satellites are observed in at least two spectral lines (such as, e.g., Ly-5 and Ly-6 lines in Fig. 3), then it is possible to find a single pair of ε_1 and ε_2 satisfying the above criterion. In particular, for this case the theoretical analysis, through variations of different plasma and laser parameters, led to the following pair: $\varepsilon_1 = 4$, $\varepsilon_2 = 1$. According to Eq. (8), this translates into the electric field amplitudes $E_1 = 14$ GV/cm, $E_2 = 7$ GV/cm.

In these shots the laser intensity was $3\text{x}10^{18}$ W/cm^2, corresponding to the electric field amplitude in vacuum $E_0 = 48$ GV/cm. Thus, the conversion efficiency, defined as the ratio of the energy density in the generated second harmonic in the plasma to the energy density of the incident laser field in vacuum, was 2%.

For fitting the experimental profiles of the Ly-delta and Ly-epsilon lines it was necessary to take into account that the observed emission is a superposition of the emission from a more dense plasma region, where there are waves t_1 and t_2, with the emission from a less dense, but a larger plasma region, where there are no periodic electric fields. In this situation the

#250983 Received 29 Sep 2015; revised 19 Nov 2015; accepted 20 Nov 2015; published 3 Dec 2015

theoretical spectrum of a line consists of a relatively broad pedestal, emitted from the periodic-field-region, and a relatively narrow, but more intense component, emitted from the no-periodic-field-region.

We mention the fact that while the electron densities of the periodic-field region and of the no-periodic-field region are noticeably different (~$3x10^{20}$ cm^{-3} and ~$1x10^{20}$ cm^{-3}, respectively, as found from the best fit to the experimental profiles), the Stark broadening by ion and electron microfields does not differ that much in these two regions as compared to how they would differ if it were not for the following phenomenon. The fairly strong field of the wave t_1 dramatically *suppresses the Stark broadening by the ion microfield* in the periodic-field region. This phenomenon was predicted theoretically in [44] and later confirmed experimentally in a tokamak plasma [45] (see also book [43] Sects. 4.3.1 and 7.5.1). Since for the hydrogenic multicharged systems the predominant mechanism of the Stark broadening is the broadening by the ion microfield, its suppression by the strong field of the wave t_1 leads to a significant narrowing of the Stark profile of each satellite from the periodic-field region. As a result, the Stark width of each satellite does not differ much from the Stark width of the emission from the no-periodic-field region.

We also took into account the theoretically expected asymmetry of the profiles. For the theory of the asymmetry we could refer to papers [46,47] and references therein.

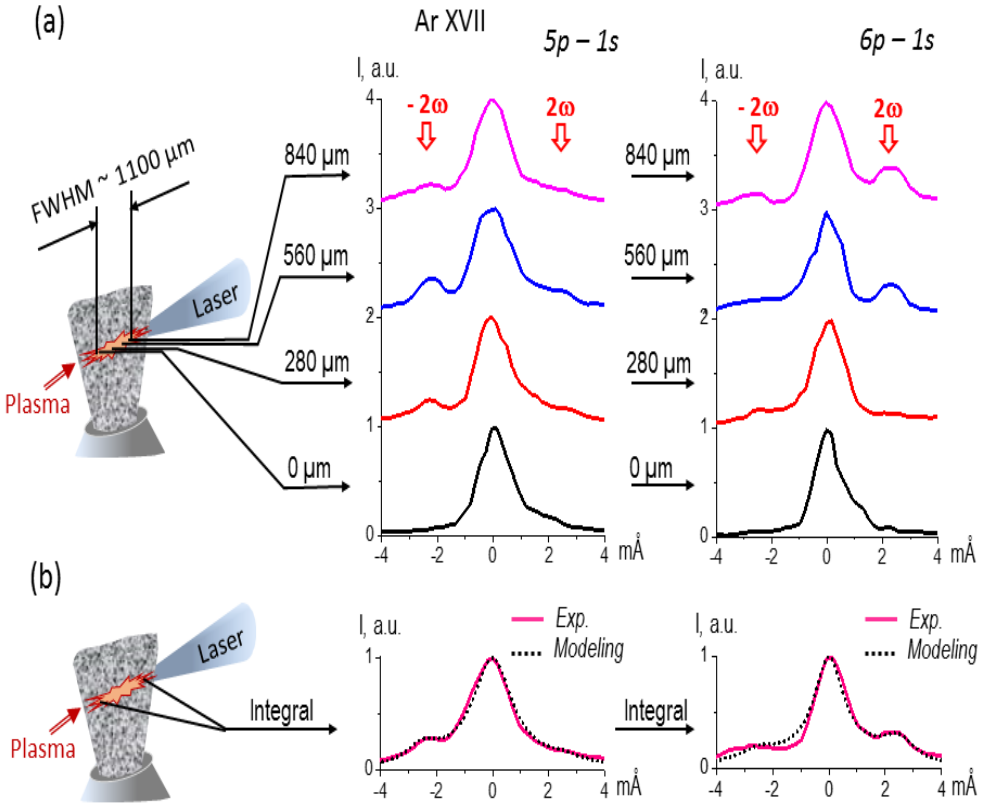

Fig. 4. Experimental and theoretical spectra of the lines Ar XVII Ly-delta (Ly-5) and Ly-epsilon (Ly-6), obtained at laser intensity ~$3x10^{18}$ W/cm^2. (a) Spatially (~280 μm)-resolved experimenttal spectra along the laser beam propagation. The most pronounced 2ω satellites are observed close to the center of plasma channel; (b) Spatially-integrated experimental spectra (solid red), for which the modeling (dashed black) was provided. There is a good agreement of the experimental and modeled results.

#250983 Received 29 Sep 2015; revised 19 Nov 2015; accepted 20 Nov 2015; published 3 Dec 2015

In addition we clarify that the Doppler and the opacity broadenings were also taken into account. However, the opacity broadening very significantly decreases as the principal quantum number n increases. Therefore, the ratio of the Stark broadening (which scales as $\sim n^2$) to the opacity broadening decreases very dramatically as n increases. The Doppler broadening is practically independent of n, so that the ratio of the Stark broadening to the Doppler broadening scales as $\sim n^2$ and rapidly increases with n. for these reasons, the Stark broadening of the lines from the levels n = 5, 6, and 7 predominated over the Doppler and opacity broadenings (though the latter two broadenings were taken into account).

Figure 3 shows the theoretical profiles providing the best fit to the corresponding experimental profiles under laser intensity 3×10^{18} W/cm^2. It is seen that the bi-chromatic field, taken into account via our newly developed theory, yields a reliable interpretation of the experimental data. The average root-mean-square deviation of the simulated profiles from the corresponding experimental profiles is less than 5%.

We emphasize that the dominance of the 2nd satellites in the spectrum of just one line could be explained by a monochromatic field. However, the dominance of the 2ω satellites in the spectra of two lines (Ly-5 and Ly-6) can be explained only by a bi-chromatic field.

For clarity: the "laser" satellites are much more intense for hydrogenic spectral lines compared to non-hydrogenic spectral lines. Therefore, under the conditions of our experiment we did not observe the 2ω satellites in lines from n = 3 and 4. As for the hydrogenic line from n = 7, at the possible location of the 2ω satellites, the intensity of this spectral line declined (compared to the center of the line) to the level close to the level of noise, so that there is zero or little visibility of the 2ω satellites.

We would like to mention that 2ω satellites could be clearly seen not only in spatially-integrated spectra presented in Fig. 3, but also in the spectra spatially-resolved (~280 μm resolution) along the laser beam propagation in the Ar cluster media, as presented in Fig. 4. It shows that 2ω satellites practically disappear at the entrance of the laser beam in the plasma and at the exit of the laser beam from the plasma, while 2ω satellites are very pronounced in the central part of the plasma, where the laser beam intensity reaches its maximum. (In Fig. 4 we do not show the spatially resolved spectra of 7p-1s line because its intensity is very low at each spatial "slice" of the plasma and only the spatially-integrated spectrum of this spectral line presents meaningful data, as shown in Fig. 3)

Figure 5 shows (in dashed blue) the experimental spectra of the lines Ar XVII Ly-5 and

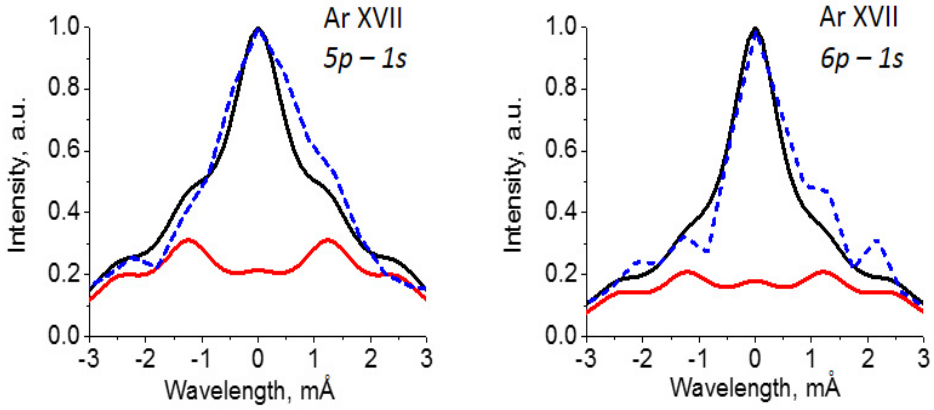

Fig. 5. Comparison of experimental and theoretical spectra of the lines Ar XVII Ly-5 and Ly-6, obtained under laser intensity 4×10^{17} W/cm^2 and laser pulse duration 500 fs (JLITE-X laser facility), with modeled ones. Dashed blue – experimental spectra, solid red at the bottom – theoretical spectra from the *monochromatic* field region (the field is $E_1 \cos(\omega t)$, E_1 = 10.6 GV/cm), solid black – total theoretical spectra, including the region of no monochromatic field.

#250983 Received 29 Sep 2015; revised 19 Nov 2015; accepted 20 Nov 2015; published 3 Dec 2015

Ly-6 obtained at the laser intensity $4x10^{17}$ W/cm^2, which is an order of magnitude lower than the laser intensity discussed in previous Fig. 3. From the theoretical analysis it turned out that these experimental profiles do *not* show a signature of the SHG. These profiles can be fitted by using just the *monochromatic* (not bi-chromatic) field at the laser frequency, as shown in Fig. 5. The average root-mean-square deviation of the simulated profiles from the corresponding experimental profiles is less than 10%.

The above does not mean that at the laser intensity $4x10^{17}$ W/cm^2, there was absolutely no SHG. Rather it means that if SHG was present, its amplitude was too small to be detected via spectral line profiles. Thus, it seems that the laser intensity threshold for SHG, deduced from the spectroscopic analysis of above spectra presented in Fig. 5 is about $4x10^{17}$ W/cm^2 or slightly smaller.

4. PIC simulations

In addition to the parametric processes (discussed in our paper just as examples) generating the second harmonic of the laser radiation, there are other nonlinear mechanisms capable of producing harmonics in laser plasmas at high laser intensity (see, e.g., paper [48]). Because of the complexity of these processes, we performed the simulations of the interaction of a short pulse of the intense linearly-polarized laser radiation with clusters of a large diameter using a 2D Particle in Cell (PIC) code [49,50] under the conditions close to our experiments. It was done by a modified 2D LSP-code [49] employing 30 particles in a cell of the size 4 nm times 4 nm and using a simulation box of the size 20 μm times 20 μm. The laser intensity was chosen as $3x10^{18}$ W/cm^2 with the pulse duration of 40 fs and the focal spot size of 4 microns. The Ar^{+16} cluster had the diameter of 500 nm and the density of 10^{22} cm^{-3}. The results of the simulations are shown in Fig. 6.

One can see in Fig. 6(a) the strong modification ("quasi-spherical" waves) of the initial laser pulse ("plane" waves) at the propagation through the cluster. The scattered light contains harmonics of the incident light. The conversion efficiency into the second harmonic was found to be about 2%, which is in excellent agreement with the result obtained by X-ray spectroscopic measurements and theoretical modeling.

Figure 6(a) shows also that harmonics propagate at a relatively small angle (about 10 degrees)

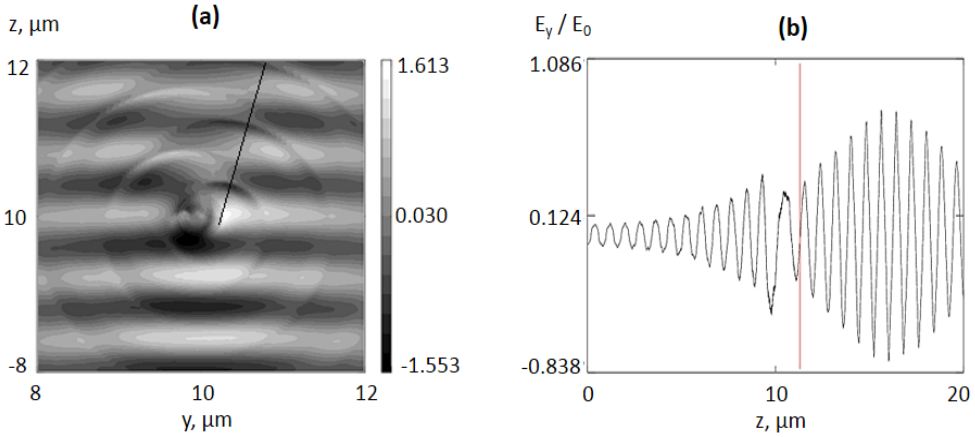

Fig. 6. Simulation of the interaction of a 40 fs pulse of intense ($3x10^{18}$ W/cm^2) linearly-polarized laser radiation with the Ar^{+16} cluster of the diameter 500 nm using a 2D PIC code. (a) The 2D spatial distribution of electric field $E_y(y,z)$ at t = 42 fs. The laser pulse propagated from bottom to the top of the figure along the z-axis. The cluster center is located at the point z = y = 10 μm. (b) The distribution of electric field $E_y(y, z)$ for y = 10 μm at t = 64 fs.

#250983 Received 29 Sep 2015; revised 19 Nov 2015; accepted 20 Nov 2015; published 3 Dec 2015

with respect to the direction of the laser beam. This is consistent with the geometry of the experiment presented in Fig. 2.

We considered the area (see red line in Fig. 6(b)) at z > 11.4 μm to avoid influence of the the ambipolar electric field. It is seen that after the propagation of laser pulse through the cluster, the initial monochromatic field is getting harmonics of the fundamental frequency. The spectrum has only a weak dependence on the position of this line.

Our PIC simulations show that there is a significant decrease of harmonics amplitude a_h with the increase of the cluster diameter r_c as $a_h \sim r_c^{-6}$. The conversion in harmonics considerably decreases with the increase of the plasma density scale length $L_n = c_s t_{Lp}$ (i.e. contrast) till the value equal to the amplitude of the electron oscillations in a laser field: $r_E = eE/m\omega^2$. Here c_s[cm/s] = $10^6 T^{1/2}$ is the ion acoustic velocity, the temperature of cold electrons is T[eV], and the duration of a laser prepulse is t_{Lp}. For the contrast 10^8 or the prepulse intensity of 3x10^{10} W/cm^2 the temperature of cold electrons is about T = 10 eV at the duration of the laser prepulse of t_{Lp} = 10 ps. From here one can get L_n = 300 nm, but in the case of the higher contrast 10^{10} this scale is 10 times less. At our laser intensity, we have r_E = 150 nm – therefore, in the case of the first contrast, the harmonics will be suppressed in comparison to the second one if the laser absorption is similar. Of course, for even lower laser contrast ~10^5, no 2ω harmonics should be produced in cluster media even for clusters of a large size, which is in a good agreement with the spectra presented in Fig. 7(a), where in such case no 2ω laser satellites were observed.

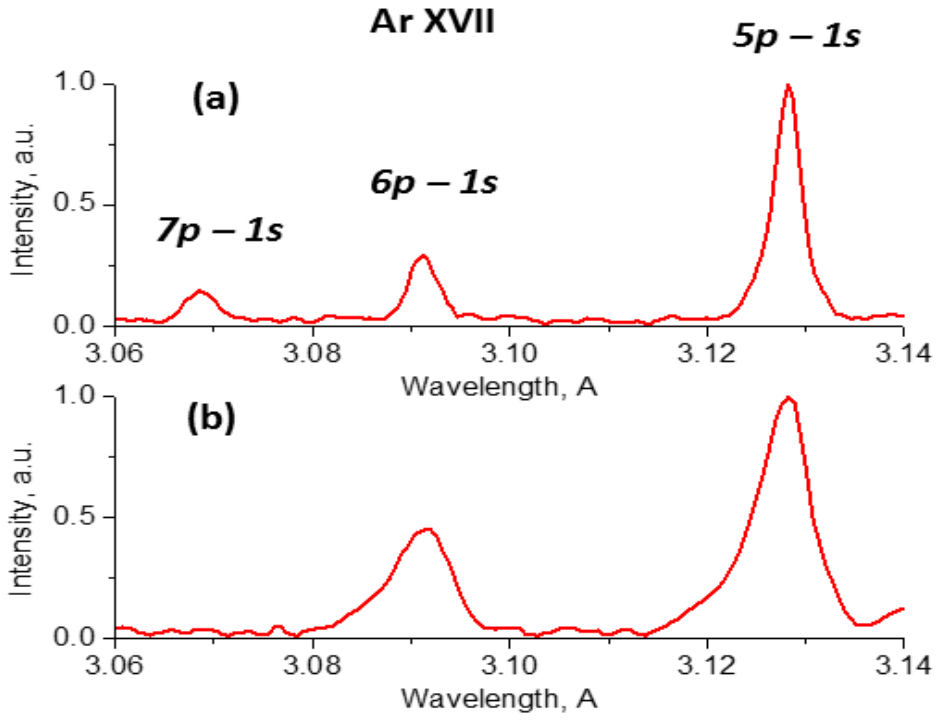

Fig. 7. Experimental spectra of the lines Ar XVII Ly-delta (Ly-5), Ly-epsilon (Ly-6), and Ly-zeta (Ly-7), obtained while decreasing either the laser intensity, or the laser contrast, or the cluster sizes. (a) Laser intensity = 1.8· 10^{18} W/cm^2, pulse duration = 30 fs, contrast = 10^5, cluster size > 1 μm[26]; (b) Laser intensity = 1· 10^{17} W/cm^2, pulse duration = 45 fs, contrast = 10^5, cluster size ~70 nm. It is seen that no 2ω laser satellites were observed, which is in a good agreement with the PIC simulation results for lower laser intensities, or lower contrasts, or smaller sizes of the clusters.

#250983 Received 29 Sep 2015; revised 19 Nov 2015; accepted 20 Nov 2015; published 3 Dec 2015

Our PIC simulations also show that at significantly lower laser intensities there was practically no harmonics generation. The threshold was found to be of the order of ~10^{17} W/cm^2 because this nonlinear process requires a relativistic laser intensity. This PIC simulation result is in a good agreement with the analysis of the experimental spectra observed at lower laser intensities of (1-4)x10^{17} W/cm^2. Indeed, there are no 2ω satellites in the experimental spectral lines presented in Fig. 7(b); there was no need to engage the bi-chromatic field for interpreting the experimental spectral lines presented in Fig. 5. The conclusion, based on the analysis of the experimental lineshapes, that there is no second harmonic generation for lower laser intensities, or lower contrasts, or smaller sizes of the clusters, is in a good agreement with the PIC simulation results.

5. Conclusions

In the experiments, where the intense femtosecond laser radiation interacted with clusters, we revealed the nonlinear phenomenon of the second harmonic generation (SHG) in the cluster-based plasma using the nonlinear phenomenon of the satellites of spectral lines of Ar XVII. This opens up the way for diagnosing the SHG in laser-produced plasma by analyzing the shapes of the emitted spectral lines.

From such lineshape analysis we found, in particular, that the efficiency of converting the short (40 fs) intense (3x10^{18} W/cm^2) incident laser light into the second harmonic was 2%. This result is in the excellent agreement with the 2D PIC simulation that we also performed. There is also a good match of the SHG threshold found from the line shape analysis and from the 2D PIC simulations.

On the experimental side, the novelty of our work is observing the X-ray spectroscopic signature of the second harmonic generation in a cluster-based plasma produced by a femtosecond laser. On the theoretical side, we developed the first ever theory of satellites of lateral Stark components in the bi-chromatic field and of satellites of the central Stark components.

Our results should be important simultaneously for several areas of physics*:* atomic physics, plasma physics, laser-plasma interactions, and physics of clusters.

Acknowledgments

The authors thank the J-KAREN and JLITE-X laser operation teams for the support. This work was supported by the Funding Program for Next Generation World-Leading Researchers (NEXT Program) from JSPS, a Grant-in-Aid for Scientific Research (A) No. 26247100 by JSPS, and the Consortium for Photon Science and Technology (CPhoST) program by MEXT. This work was also partly supported by the RFBR research projects #14-22-02089, 14-07-00863 and 14-02-91171-GFEN_a. A.A. gratefully acknowledges the computing time granted by NIC and provided on the supercomputer JUROPA at JSC.

#250983 Received 29 Sep 2015; revised 19 Nov 2015; accepted 20 Nov 2015; published 3 Dec 2015